Supplement to "Modeling of HCHO and CHOCHO at a semi-rural site in southern China during the PRIDE-PRD2006 campaign"

December 4, 2013

X. Li[1,2], F. Rohrer[1], T. Brauers[1], A. Hofzumahaus[1], K. Lu[1,*], M. Shao[2], Y. H. Zhang[2], and Andreas Wahner[1]

[1] Institut für Energie- und Klimaforschung Troposphäre (IEK-8), Forschungszentrum Jülich, Jülich, Germany
[2] College of Environmental Sciences and Engineering, Peking University, Beijing, China
[*] now at College of Environmental Sciences & Engineering, Peking University, Beijing, China

Table S1: Instrumentation for atmospheric trace gas, aerosol, and meteorology measurements at the Back Garden supersite.

Parameter	Technique	Time Res.	Accuracy	Position	Reference
HCHO, CHOCHO	MAX-DOAS	1 h	35%	hotel roof	Li et al. (2013)
OH	LIF [1]	1 min	20%	container roof	Lu et al. (2012)
O_3	UV [2]	1 min	5%	container roof	Hofzumahaus et al. (2009)
NO	CL [3]	1 min	7%	hotel roof	Hofzumahaus et al. (2009)
NO_2	Photolytic converter + CL [3]	1 min	13%	hotel roof	Hofzumahaus et al. (2009)
HONO	LOPAP [4]	5 min	10%	container roof	Li et al. (2012)
CO	NDIR [5]	1 min	5%	hotel roof	Hofzumahaus et al. (2009)
CH_4	FTIR [6]	10 min	4%	hotel roof	Lu et al. (2012)
C_2H_2, C_2H_4, C_2H_6	Offline GC-FID/MS [7]	15 min	5 – 10%	hotel roof	Liu et al. (2008)
C3 – C12 NMHCs	Online GC-FID	1 h	10%	hotel roof	Wang et al. (2008)
H_2O_2, CH_3OOH	Online HPLC	20 – 60 min	10%	hotel roof	Hua et al. (2008)
PAN, PPN	Online GC-ECD	5 min	15%, 20%	hotel roof	Wang et al. (2010)
S_a [a]	TDMPS-APS [8]	10 min	10 – 30%	hotel roof	Yue et al. (2010)
Aerosol composition [b]	Q-AMS	10 min	14%	hotel roof	Hu et al. (2012)
Black carbon	MAAP [9]	2 min	10%	hotel roof	–
Photolysis frequency	SR [10]	1 min	10%	hotel roof	Bohn et al. (2008)
Temperature	USA [11]	10 min	0.3 K	container roof	Li et al. (2012)
Pressure	Vaisala WXT510	10 min	0.5 hPa	hotel roof	Li et al. (2012)
Relative humidity	Vaisala WXT510	10 min	3%	hotel roof	Li et al. (2012)
Wind speed	USA [11]	10 min	$0.1\,m\,s^{-1}$	container roof	–
Wind direction	USA [11]	10 min	0.1 °	container roof	–

[a]: Aerosol surface concentration for aerosols with diameter of 3 nm – 10 μm. [b]: Organic matter and inorganic ions (sulfate, nitrate, ammonium, and chloride) of aerosols with diameter less than 1 μm.

[1]: Laser Induced Florescence. [2]: Ultraviolat absorption instrument (Thermo Electron, model 49C). [3]: Chemiluminescence instrument (Thermo Electron, model 42CTL). [4]: Long-path absorption photometry. [5]: Non-Dispersive Infrared gas analyzer (Thermo Electron, Model 48C). [6]: Fourier-transform infrared spectrometry. [7]: Canister sampling followed by GC-FID/MS analysis. [8]: Twin Differential Mobility Particle Sizer and Aerodynamic Particle Sizer. [9]: Multi-angle absorption photometer (Thermo Electron MAAP5012). [10]: Spectral radiometry. [11]: Ultra sonic anemometer (USA-1, Metek, Germany).

Table S2: Model scenarios used in the sensitivity study of HCHO and CHOCHO simulation during the PRIDE-PRD2006 campaign.

Simulation	Mechanisms	Purpose
M0	MCM v3.2 with $\tau_D = 24$ h	Base run
MS1	as M0, but using different OH concentrations	Sensitivity of HCHO and CHOCHO on OH level
MS2	as M0, but using different NMHCs concentrations	Sensitivity of HCHO and CHOCHO on NMHCs level
MS3	as M0, but using different NO and NO_2 concentrations	Sensitivity of HCHO and CHOCHO on NO_X level
MS4	as M0, with measured H_2O_2 and CH_3OOH concentrations as additional model constraints	Sensitivity of HCHO and CHOCHO on H_2O_2 and CH_3OOH
MS5	as M0, with measured PAN and PPN concentrations as additional model constraints	Sensitivity of HCHO and CHOCHO on PANs
MS6	as M0, but using different values of τ_D	Sensitivity of HCHO and CHOCHO on the flushing-out of all species in the model

Table S3: Estimated uncertainties of model input parameters and reaction rate constant.

Input parameter	Uncertainty factor
j [a]	$\times\,1.1$
τ_D	$\times\,2$
T	$\times\,1.005$
P	$\times\,1.005$
OH	$\times\,1.2$
H_2	$\times\,1.2$
CO	$\times\,1.05$
NO	$\times\,1.07$
NO_2	$\times\,1.13$
O_3	$\times\,1.05$
H_2O	$\times\,1.1$
HONO	$\times\,1.1$
CH_4	$\times\,1.04$
Ethane [b]	$+\,1$ ppb
Ethene [b]	$+\,2$ ppb
Ethyne [b]	$+\,1$ ppb
C3–C12 NMHCs	$\times\,1.2$
k_i [c]	$\times\,1.3$

[a] The errors of the measured photolysis frequencies are assumed to be correlated since they were derived from the same measurement of the solar actinic flux.
[b] Campaign averaged values were applied for ethane, ethene, and ethyne, so that the standard deviation of the canister samples were propagated as uncertainties rather than the measurement accuracy.
[c] All the reaction constants of non-photolytic reactions in MCM v3.2 are estimated to have 30% accuracy (1σ).

Figure S1: Mean diurnal variation of the uncertainty of the modeled HCHO and CHOCHO concentrations by the model base-case (M0). The red, blue, and pink lines represent the error originated from the uncertainty of physical parameters (i.e., photolysis frequencies, deposition lifetime, T, P), radical and trace gas concentrations, and reaction rate constants of non-photolytic reactions in the model. The black lines are the sum of the above three errors.

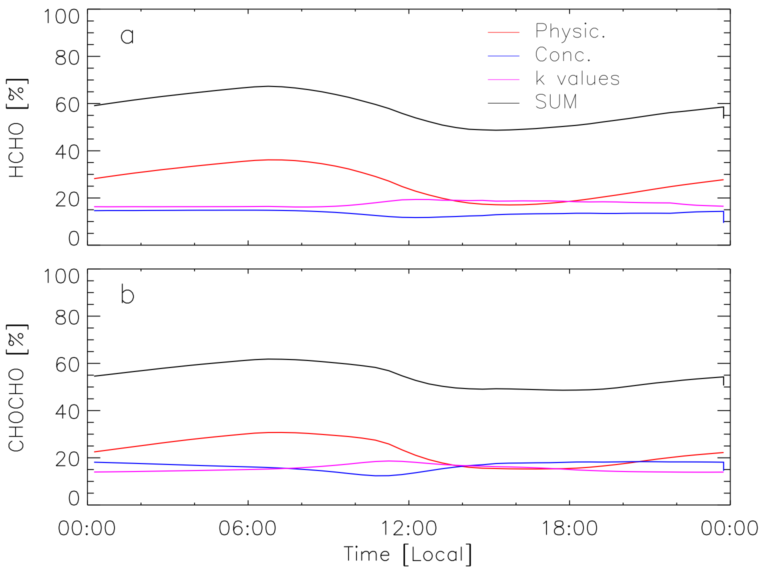

Figure S2: Measured and modeled HCHO and CHOCHO concentrations in the 6 cloud-free days during the PRIDE-PRD2006 campaign. The black "△" and the error bar refers to the measured concentration and the measurement error, respectively. The red "○" presents results of the model base-case (i.e., M0). The symbols "×" represent results of models constrained by different OH concentrations, i.e., model MS1 as described in the paper.

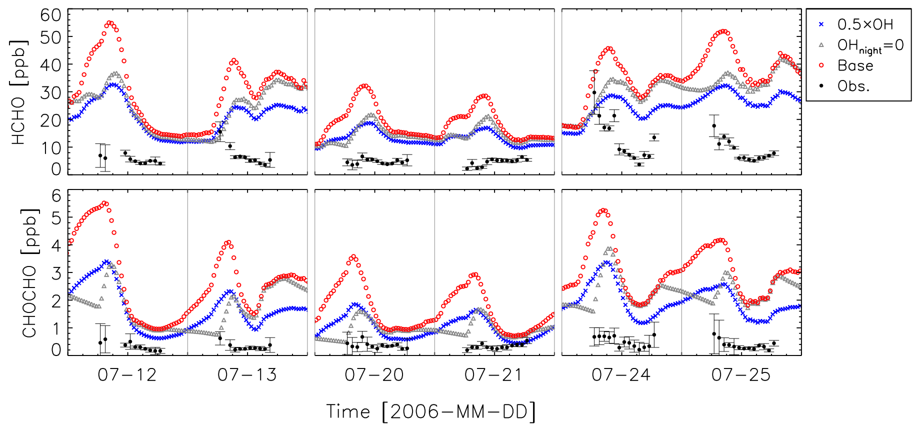

Figure S3: Measured and modeled HCHO and CHOCHO concentrations in the 6 cloud-free days during the PRIDE-PRD2006 campaign. The black "•" and the error bar refers to the measured concentration and the measurement error, respectively. The red "∘" presents results of the model base-case (i.e., M0). The symbols "×" represent results of models constrained by different NMHCs concentrations, i.e., model MS2 as described Table S2. Iso* represents the model scenario in which the isoprene concentration between 8:00 − 16:00 is constrained by 52% of the measured value.

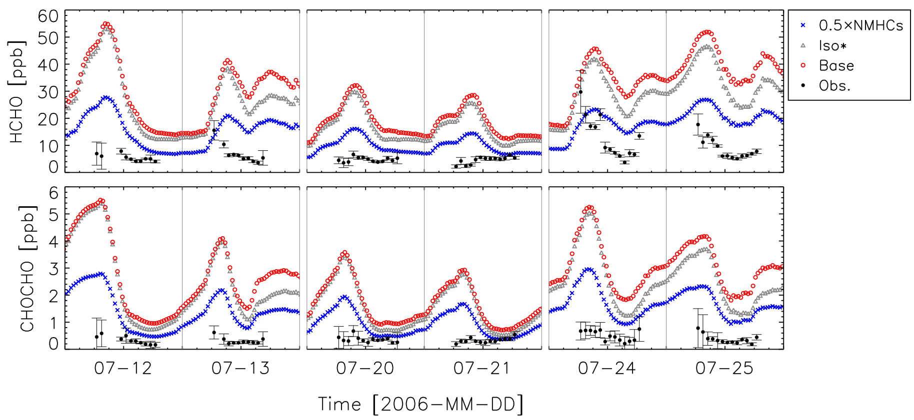

Figure S4: Measured and modeled HCHO and CHOCHO concentrations in the 6 cloud-free days during the PRIDE-PRD2006 campaign. The black "•" and the error bar refers to the measured concentration and the measurement error, respectively. The red "○" presents results of the model base-case (i.e., M0). The symbols "×" represent results of models constrained by different H_2O_2 (HP) and CH_3OOH (MHP) concentrations, i.e., model MS4 as described in Table S2.

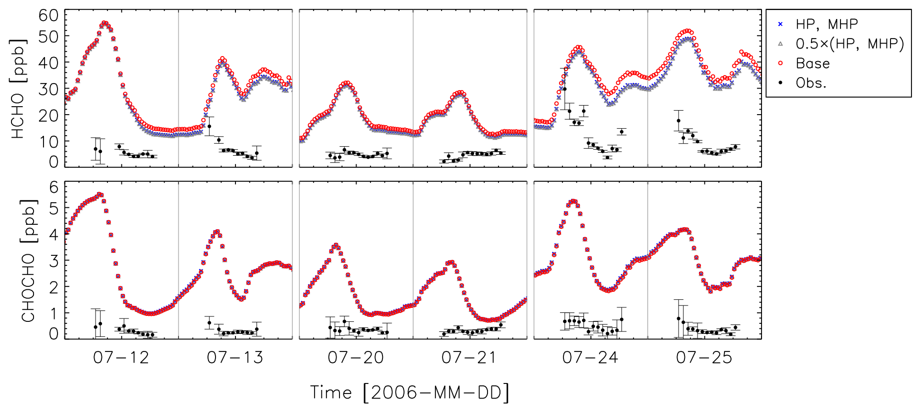

Figure S5: Measured and modeled HCHO and CHOCHO concentrations in the 6 cloud-free days during the PRIDE-PRD2006 campaign. The black "•" and the error bar refers to the measured concentration and the measurement error, respectively. The red "∘" presents results of the model base-case (i.e., M0). The symbols "×" represent results of models constrained by different PANs (PAN, PPN) concentrations, i.e., model MS5 as described in Table S2.

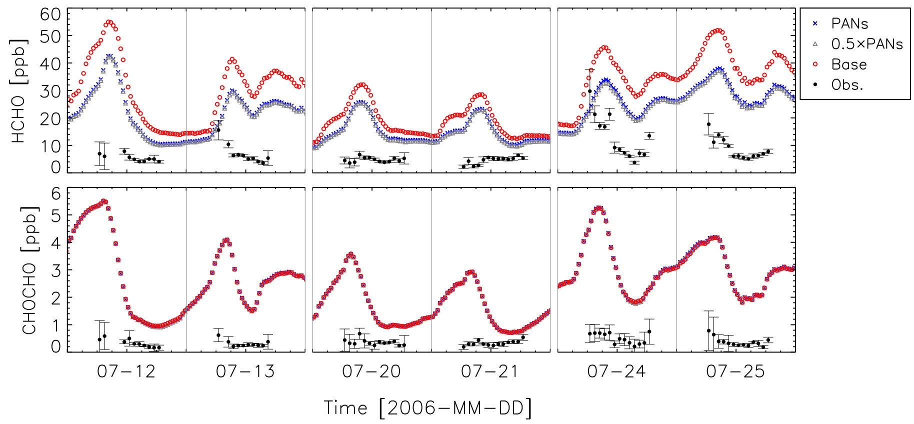

Figure S6: Measured and modeled HCHO and CHOCHO concentrations and total OH reactivity in the 6 cloud-free days during the PRIDE-PRD2006 campaign. The black "•" and the error bar refers to the measured value and the measurement error, respectively. The red "○" presents results of the model base-case (i.e., M0). The symbols "×" represent results of models constrained by different values of flushing-out parameter (τ_D), i.e., model MS6 as described in Table S2.

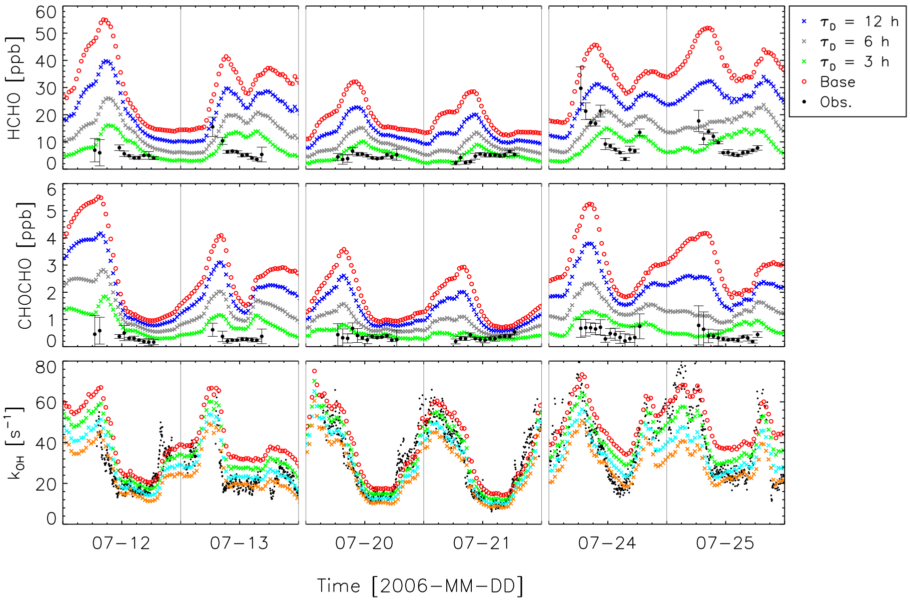

References

Bohn, B., Corlett, G. K., Gillmann, M., Sanghavi, S., Stange, G., Tensing, E., Vrekoussis, M., Bloss, W. J., Clapp, L. J., Kortner, M., Dorn, H. P., Monks, P. S., Platt, U., Plass-Dlmer, C., Mihalopoulos, N., Heard, D. E., Clemitshaw, K. C., Meixner, F. X., Prevot, A. S. H., and Schmitt, R.: Photolysis frequency measurement techniques: results of a comparison within the ACCENT project, Atmos. Chem. Phys., 8, 5373–5391, doi:10.5194/acp-8-5373-2008, 2008.

Hofzumahaus, A., Rohrer, F., Lu, K., Bohn, B., Brauers, T., Chang, C.-C., Fuchs, H., Holland, F., Kita, K., Kondo, Y., Li, X., Lou, S., Shao, M., Zeng, L., Wahner, A., and Zhang, Y.: Amplified Trace Gas Removal in the Troposphere, Science, 324, 1702–1704, doi:10.1126/science.1164566, 2009.

Hu, W. W., Hu, M., Deng, Z. Q., Xiao, R., Kondo, Y., Takegawa, N., Zhao, Y. J., Guo, S., and Zhang, Y. H.: The characteristics and origins of carbonaceous aerosol at a rural site of PRD in summer of 2006, Atmos. Chem. Phys., 12, 1811–1822, doi:10.5194/acp-12-1811-2012, 2012.

Hua, W., Chen, Z. M., Jie, C. Y., Kondo, Y., Hofzumahaus, A., Takegawa, N., Chang, C. C., Lu, K. D., Miyazaki, Y., Kita, K., Wang, H. L., Zhang, Y. H., and Hu, M.: Atmospheric hydrogen peroxide and organic hydroperoxides during PRIDE-PRD'06, China: their concentration, formation mechanism and contribution to secondary aerosols, Atmos. Chem. Phys., 8, 6755–6773, doi:10.5194/acp-8-6755-2008, 2008.

Li, X., Brauers, T., Häseler, R., Bohn, B., Fuchs, H., Hofzumahaus, A., Holland, F., Lou, S., Lu, K. D., Rohrer, F., Hu, M., Zeng, L. M., Zhang, Y. H., Garland, R. M., Su, H., Nowak, A., Wiedensohler, A., Takegawa, N., Shao, M., and Wahner, A.: Exploring the atmospheric chemistry of nitrous acid (HONO) at a rural site in Southern China, Atmos. Chem. Phys., 12, 1497–1513, doi: 10.5194/acp-12-1497-2012, 2012.

Li, X., Brauers, T., Hofzumahaus, A., Lu, K., Li, Y. P., Shao, M., Wagner, T., and Wahner, A.: MAX-DOAS measurements of NO2, HCHO and CHOCHO at a rural site in Southern China, Atmos. Chem. Phys., 13, 2133–2151, doi: 10.5194/acp-13-2133-2013, 2013.

Liu, Y., Shao, M., Lu, S., Chang, C.-c., Wang, J.-L., and Chen, G.: Volatile Organic Compound (VOC) measurements in the Pearl River Delta (PRD) region, China, Atmos. Chem. Phys., 8, 1531–1545, doi:10.5194/acp-8-1531-2008, 2008.

Lu, K. D., Rohrer, F., Holland, F., Fuchs, H., Bohn, B., Brauers, T., Chang, C. C., Hseler, R., Hu, M., Kita, K., Kondo, Y., Li, X., Lou, S. R., Nehr, S., Shao, M., Zeng, L. M., Wahner, A., Zhang, Y. H., and Hofzumahaus, A.: Observation and modelling of OH and HO2 concentrations in the Pearl River Delta 2006: a missing OH source in a VOC rich atmosphere, Atmos. Chem. Phys., 12, 1541–1569, doi:10.5194/acp-12-1541-2012, 2012.

Wang, B., Shao, M., Roberts, J. M., Yang, G., Yang, F., Hu, M., Zeng, L., Zhang, Y., and Zhang, J.: Ground-based on-line measurements of peroxyacetyl nitrate (PAN) and peroxypropionyl nitrate (PPN) in the Pearl River Delta, China, Intern. J. Environ. Anal. Chem., 90, 548–559, doi: 10.1080/03067310903194972, 2010.

Wang, J.-L., Wang, C.-H., Lai, C.-H., Chang, C.-C., Liu, Y., Zhang, Y., Liu, S., and Shao, M.: Characterization of ozone precursors in the Pearl River Delta by time series observation of non-methane hydrocarbons, Atmos. Environ., 42, 6233–6246, doi:10.1016/j.atmosenv.2008.01.050, 2008.

Yue, D. L., Hu, M., Wu, Z. J., Guo, S., Wen, M. T., Nowak, A., Wehner, B., Wiedensohler, A., Takegawa, N., Kondo, Y., Wang, X. S., Li, Y. P., Zeng, L. M., and Zhang, Y. H.: Variation of particle number size distributions and chemical compositions at the urban and downwind regional sites in the Pearl River Delta during summertime pollution episodes, Atmos. Chem. Phys., 10, 9431–9439, doi:10.5194/acp-10-9431-2010, 2010.